XL CILAMCE
IBERO-LATIN AMERICAN CONGRESS ON COMPUTATIONAL METHODS IN ENGINEERING
NOVEMBER 11-14, 2019
Praiamar Natal Hotel & Convention
Natal, RN-BRAZIL

COMPARATIVE ANALYSIS OF TRIGONOMETRIC ENRICHMENTS USED IN DYNAMIC ANALYSIS OF TIMOSHENKO BEAMS BY THE GENERALIZED FINITE ELEMENT METHOD

Patrícia L. M. Freisleben
patriciafreisleben@hotmail.com
Federal Technological University of Paraná
Pato Branco, 85503-390, Paraná, Brasil
Paulo de Oliveira Weinhardt
Marcos Arndt
Roberto Dalledone Machado
paulo.weinhardt@gmail.com
arndt.marcos@gmail.com
roberto.dalledonemachado@gmail.com
Federal University of Paraná
Curitiba, 81.531-980, Paraná, Brasil

Abstract. The Finite Element Method (FEM) is widely used in the dynamic analysis of structures, however it has some limitations. In order to improve the numerical response, enriching functions can be incorporated to FEM approximation space using the Generalized Finite Element Method (GFEM) procedure. Several studies have already been carried out to prove the efficiency of GFEM in the dynamic analysis of bars, Euler-Bernoulli beams, trusses, among other structural elements, but few studies have investigated the application of GFEM in the dynamic analysis of Timoshenko beams. The present work aims to contribute to this field presenting modal and transient analyses of Timoshenko beams using the GFEM technique. Three different trigonometric enrichments are used to perform modal and transient analyses of Timoshenko clamped-free beams without damping and the results are compared with those obtained by FEM. The normalized spectrum is obtained by the modal analysis and displacements, velocities and accelerations of the beam along the time are also calculated by transient analysis. In that manner the efficiency of each GFEM enrichment in modal and transient analysis of Timoshenko beams is discussed.

Keywords: Generalized Finite Element Method, Timoshenko beams, trigonometric enrichments, dynamic analysis.

1 Introduction

Dynamic phenomena are usually divided into free vibrations and forced vibrations. The first ones occur when a system, after an initial disturbance, vibrates on its own freely, that is, without external forces acting on the system. In this context, natural vibration modes and frequencies are analyzed in free vibration. This procedure is called modal analysis and has great relevance in structural dynamic analysis. Analyzing the modes and frequencies of vibration aims to characterize the structural behavior, since whenever the natural frequency of a structure or machine coincides with the frequency of external excitation, a phenomenon known as ressonance occurs. That generates amplification of displacements and possible damages to the structure [1, 2].

On the other side, forced vibration occurs when the system is subjected to an time-dependent external force (usually generated by a repeated force type). In a forced vibration case, the external energy can be supplied by an applied force or imposed displacement excitation. What is sought to reproduce with a forced vibration modeling is the displacements variation, as well as velocities and accelerations of the structure over time, known as structural transient responses [1].

In order to obtain the modal and transient responses, a mathematical model of the problem must be well stated and then some eficient computational modeling. A physical model is the first to be developed embedding ordem further modeling procedures from the structural system that will be analyzed. In this sequence, it is performed the mathematical modeling where the physical model is described in terms of equations to be applied to the computational model. The equations of motion must be solved to find the responses of the vibration system, and for this, among several techniques, numerical methods can be used [1, 3].

Some numerical methods can be used to solve those problems numerically. Among them, one can refer to the Finite Element Method (FEM) [4–6], to the Differential Quadrature Method (DQM) [7, 8] and to the Method of Isogeometric Analysis [9]. Among those, FEM is widely used in the industry to model structural vibration problems, despite its limitations [10].

The FEM technique consists of dividing the solution region, also called the solution domain, into small parts known as elements and expressing the unknown field variables in terms of assumed approximation functions, also known as interpolation functions or shape functions, in each element. Shape functions are defined in field variables of specified points designated by nodes or nodal points. Thus, in finite element analysis, the unknown variables are the field variables of the nodal points. Once these are calculated, the field variables at any point can be found using the shape functions to interpolate the seeked field [11].

The technique requires, among other things, a continuity between the elements, because in this way the local unknowns are interconnected, generating a solvable global system. This requirement historically discouraged the use of non-polynomial fucntions and a variety of approaches have been suggested to create finite element spaces that contain non-polynomial functions and satisfy some form of continuity between elements [12].

One approach, proposed by Melenk [13], presents a method where local approximation spaces are multiplied by a Partition of Unit to build the global approximation space. This approach was modified by Melenk [12] embeddeding it mathematically. This new approach was later called Partition of Unit Method (PUM). As a consequence of the applied methodologies, the approximation properties of the local spaces are inherited by the global space of finite elements [12], allowing to take advantage of prior knowledge of the problem to enrich the approximation space.

The FEM is a conforming method, however, it does not present the ability to systematically explore prior knowledge about the problem to be solved. If it is necessary to use custom functions it is necessary to reconstruct a computational model for each application. Therefore, to solve this issue, the Generalized Finite Element Method (GFEM) can be used. GFEM is a method in which special functions are multiplied by partition of unit of the PUM, without the need to reconstruct the whole model [14].

Another GFEM feature is that special functions and finite element functions can be mixed in the approximation, and used only when necessary. The only difficulty presented for this implementation of GFEM is that the functions used in the construction of the approximation should not be linearly dependent or almost linearly dependent [14].

The GFEM has already presented good results in the dynamic analysis of bars; Euler-Bernoulli beams; trusses; frames; two-dimensional wave equation; plane stress state; and, curved beams [2, 15–21].

However, few studies have investigated the application of GFEM in the dynamic analysis of Timoshenko beams [22–24]. This beam theory proposed by Timoshenko [25] includes the rotation inertia and shear deformation to the Euler-Bernoulli beam model. Timoshenko's model brings a great improvement to non-thin beams and high frequency responses in which the shear or rotationary effects are not negligible [25].

In this escope, this work aims to contribute with the investigation of modal and transient analyses of Timoshenko beams applying the GFEM. This work use three different trigonometric enrichments to perform modal and transient analyses of Timoshenko clamped-free beams without damping, comparing their results with those obtained by FEM.

2 Timoshenko finite element beam model

Firstly, it's important to note that will be used the approach presented in the work of Hsu [22] to obtain the mass and stiffness matrices.

Considering the dynamic equilibrium equation of Timoshenko beams in free vibration, based on the principle of virtual work, the weak form of the equation can be written as [26]:

$$\int_0^l EI\frac{\partial \phi}{\partial x}\delta\frac{\partial \phi}{\partial x}dx+\int_0^l k_sGA\left(\frac{\partial y}{\partial x}-\phi\right)\delta\left(\frac{\partial y}{\partial x}-\phi\right)dx=\int_0^l \delta y\rho A\frac{\partial^2 y}{\partial t^2}dx+\int_0^l \delta\phi\rho I\frac{\partial^2 \phi}{\partial t^2}dx, \quad (1)$$

where l denotes total beam length, E denotes the modulus of longitudinal elasticity, I denotes moment of inertia, ϕ is the rotation, δ denotes that the terms are virtual, k_s is the shear correction factor, G is the transverse modulus of elasticity, A is the cross sectional area, y is the displacement and ρ is the density of material.

The discretization of Eq. (1) can be made by unidirectional linear finite elements, with two nodes and two degrees of freedom at each node, namely transverse displacement and in-plane rotation. The approximated solution in the displacement field is given by:

$$y(x)=\sum_{i=1}^{n} y_i\gamma_i(x), \quad (2)$$

$$\phi(x)=\sum_{i=1}^{n} \phi_i\gamma_i(x), \quad (3)$$

where y_i denotes the i-th displacement ϕ_i is the i-th rotation and γ_i is the i-th shape functions.

Considering the natural coordinate $\xi=[-1,1]$ in the element domain, the approximated solution in the field of displacements can be expressed using linear shape functions:

$$y(\xi)=y_1\gamma_1(\xi)+y_2\gamma_2(\xi), \quad (4)$$

$$\phi(\xi)=\phi_1\gamma_1(\xi)+\phi_2\gamma_2(\xi). \quad (5)$$

They can be expressed in matrix form as:

$$y(\xi) = [H_y]\,\{w\}, \tag{6}$$

$$\phi(\xi) = [H_\phi]\,\{w\}, \tag{7}$$

where $[H_y]$ is the matrix of displacement shape functions, $[H_\phi]$ is the matrix of rotation shape functions and $\{w\}$ is the nodal displacement vector, given by:

$$[H_y] = \begin{bmatrix} \gamma_1 & 0 & \gamma_2 & 0 \end{bmatrix}, \tag{8}$$

$$[H_\phi] = \begin{bmatrix} 0 & \gamma_1 & 0 & \gamma_2 \end{bmatrix}, \tag{9}$$

and

$$\{w\} = \begin{Bmatrix} u_1 \\ \phi_1 \\ u_2 \\ \phi_2 \end{Bmatrix}. \tag{10}$$

After replacing Eq. (2) and Eq. (3) in Eq. (1), it is possible to determine the mass matrix, $[M^e]$ and stiffness matrix in the element domain, $[k^e]$,

$$[k^e] = \int_{-1}^{1} [B]^T [D][B] |J| d\xi, \tag{11}$$

$$[M^e] = \int_{-1}^{1} (\rho A)[H_y]^T [H_y] |J| d\xi + \int_{-1}^{1} (\rho I)[H_\phi]^T [H_\phi] |J| d\xi, \tag{12}$$

where $[B]$ is the deformation matrix, $[D]$ is the constitutive matrix and $|J|$ is the Jacobian determinant, given by:

$$[B] = \begin{bmatrix} 0 & \frac{1}{|J|}\left(\frac{d\gamma_1}{d\xi}\right) & 0 & \frac{1}{|J|}\left(\frac{d\gamma_2}{d\xi}\right) \\ \frac{1}{|J|}\left(\frac{d\gamma_1}{d\xi}\right) & -\gamma_1 & \frac{1}{|J|}\left(\frac{d\gamma_2}{d\xi}\right) & -\gamma_2 \end{bmatrix}, \tag{13}$$

$$[D] = \begin{bmatrix} EI & 0 \\ 0 & k_s GA \end{bmatrix}. \tag{14}$$

After proper algebraic manipulations in Eq. (1) and considering that the nodal displacement vector can be expressed by $w = \Phi_n e^{i\omega_n t}$, Eq. (1) can be expressed as a quadratic matrix eigenvalue problem

$$[\mathbf{K} - \omega_n^2 \mathbf{M}]\Phi_n = 0, \tag{15}$$

where ω_n are the natural frequencies and Φ_n are the vibration modes.

The frequencies obtained from Eq. (15) will be dimensionless by:

$$\beta_n^2 = \omega_n l^2 \sqrt{\frac{\rho A}{EI}}, \tag{16}$$

where β_n are approximated dimensionless eigenvalues.

3 Generalized finite element method

The approximated solution proposed by the GFEM can be written as a combination of the components [27]:

$$y^h(\xi) = y^h_{FEM} + y^h_{GFEM}. \tag{17}$$

The FEM shape functions used in this work are the linear Lagrange polynomials given by:

$$\gamma_1 = \frac{1-\xi}{2}, \tag{18}$$

$$\gamma_2 = \frac{1+\xi}{2}, \tag{19}$$

with domain $\xi = [-1, 1]$.

As stated earlier, the solution approach is a combination of components presented in Eq. (17). The FEM component is then given by:

$$y^h_{FEM}(\xi) = \sum_{i=1}^{2} \gamma_i(\xi) y_i. \tag{20}$$

Lagrange's linear functions also form a partition of unit. Therefore, these functions will also be used as a partition of unity in GFEM displacement component, such as:

$$\eta_1 = \frac{1-\xi}{2}, \tag{21}$$

$$\eta_2 = \frac{1+\xi}{2}. \tag{22}$$

This paper presents three different sets of enrichment functions. The first set of enriching functions was presented by Arndt [15] for bars and is used here for comparison purposes. In Torii [2], the size of the element within the formulation proposed by Arndt [15] was removed and Weinhardt [17] presents a modification in the parameter β_j. The enrichment is given by Eq. (23) to Eq. (26), shown in the following form:

$$\psi_{1j} = sin(\beta_j(\xi + 1)), \tag{23}$$

$$\psi_{2j} = sin(\beta_j(\xi - 1)), \tag{24}$$

$$\phi_{1j} = \cos(\beta_j(\xi + 1)) - 1, \tag{25}$$

$$\phi_{2j} = \cos(\beta_j(\xi - 1)) - 1, \tag{26}$$

where the parameter β_j, with $j = 1, 2, 3, ..., m$ and m is the number of enrichment levels, is given by:

$$\beta_j = \pi \left(2(j - 1) + \frac{3}{4} \right). \tag{27}$$

The GFEM component of Eq. (17) for this enrichment is given by:

$$y^h_{GFEM} = \sum_{i=1}^{2} \eta_i(\xi) \left[\sum_{j=1}^{m} (\psi_{ij} a_{ij} + \phi_{ij} b_{ij}) \right], \tag{28}$$

where a_{ij} and b_{ij} are the field degrees of freedom.

The second set of enrichment functions used in this work was also presented by Arndt [15] for modelling Euler-Bernoulli beams, a more similar problem, and it is given by:

$$\psi_{1j} = \cos\left(\frac{(j - 1)\pi(\xi + 1)}{2} \right) - \cos\left(\frac{(j + 1)\pi(\xi + 1)}{2} \right), \tag{29}$$

where $j = 1, 2, 3, ..., m$.

The GFEM component of Eq. (17) for this enrichment is given by:

$$y^h_{GFEM} = \sum_{i=1}^{2} \eta_i(\xi) \left[\sum_{j=1}^{m} \psi_{1j}(\xi) a_{ij} \right]. \tag{30}$$

Finally, the third enrichment was presented by Hsu [22], for Timoshenko beams, and is given by:

$$\psi_{1j} = sin\left(\frac{\beta_j(\xi + 1)}{2} \right), \tag{31}$$

$$\psi_{2j} = sin\left(\frac{\beta_j(\xi - 1)}{2} \right), \tag{32}$$

being in this case $\beta_j = j\pi$, with $j = 1, 2, 3, ..., m$.

The GFEM component of Eq. (17) for this enrichment is given by:

$$y^h_{GFEM} = \sum_{i=1}^{2} \eta_i(\xi) \left[\sum_{j=1}^{m} \psi_{ij}(\xi) a_{ij} \right]. \tag{33}$$

4 Numerical results

In the examples presented in this section a clamped-free beam is studied. In order to illustrate this beam boundary condition, the Fig. 1 is presented. In the following examples the beam properties are $l = 1,0$; $b = 1,0$; $E = 1,0$; $\rho = 1,0$; $k_s = 5/6$; $\nu = 0,3$; $G = E/(2(1 + \nu))$; $A = bh$; $I = (bh^3)/12$ e $l_e = l/N_{elem}$, where b is the cross-section base of the beam, ν is the Poisson coefficient, h is the height of the cross section of the beam and N_{elem} is the total number of elements in numerical analysis.

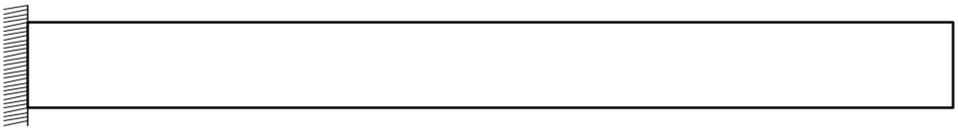

Figure 1. Clamped-free beam

It's well known that Timoshenko beams presents some shear locking effect and to overcome this problem a reduced integration is adopted for FEM analysis using Gaussian quadrature with a fixed order of one point. For the GFEM analysis the element domain was sub-divided into 10 intervals, with three numerical integration points at each interval, with no need of sub-integration procedures.

4.1 Modal analysis

The modal analysis aims to obtain the vibration frequencies of structure through the solution of the eigenproblem given in Eq. (15). The beam has a ratio between the cross-sectional height and the beam length of 0.1. This value of relation is considered high, and the shear effect must be taken into account, making Timoshenko model necessary.

Frequency results are presented by normalized frequency spectrum plots. In them, the resulting frequencies of each enrichment function set for the GFEM with five levels of enrichment are displayed. At the end, a frequency spectrum graph with the fifth level of enrichment is presented with the three sets of enrichment functions for the GFEM and the FEM frequencies.

Modal analytical solution is very difficult to obtain and therefore a reference solution using a very refined mesh FEM model was adopted. Taking into consideration that it is possible to obtain precise values for about 20% of the frequencies generated by FEM, a model with 8000 degrees of freedom was adopted so that the quantity of frequencies with good precision that can be taken by this model exceeds those obtained with the other analyzes, validating a sufficiente reliabe reference.

The spectrum, shown in Fig. 2, is for the set of enrichment functions presented by Arndt [15] for bars.

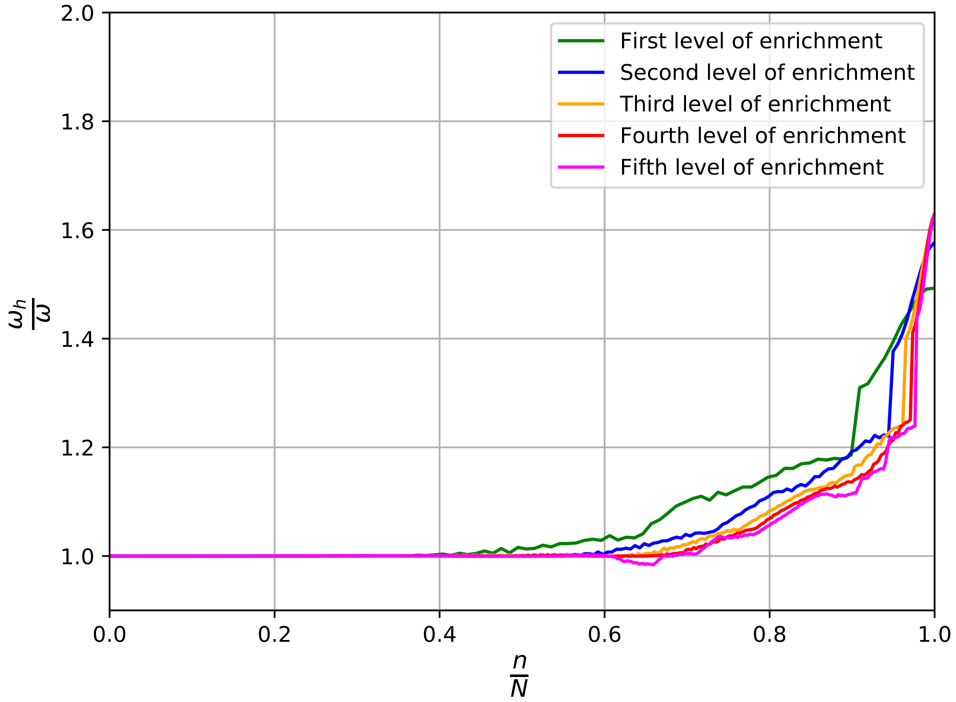

Figure 2. Enrichment Arndt [15] for bars

For a better observation, a zoom at the end of the spectrum is presented in Fig. 3.

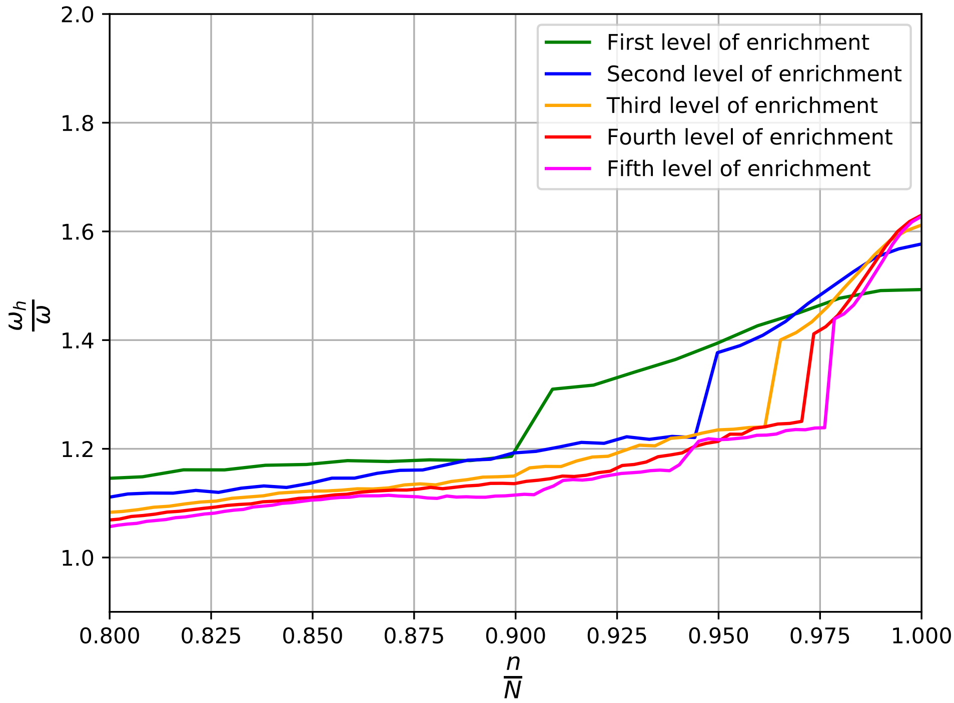

Figure 3. Zoom of enrichment Arndt [15] for bars

It is possible to observe in the frequency spectra of the enrichment presented by Arndt [15] for bars that as the level of enrichment increases the accuracy also improves. However, all enrichment levels show good frequency responses up to approximately 80% of the frequencies obtained.

The spectrum, shown in Fig. 4, is for the set of enrichment functions presented by Arndt [15] for beams.

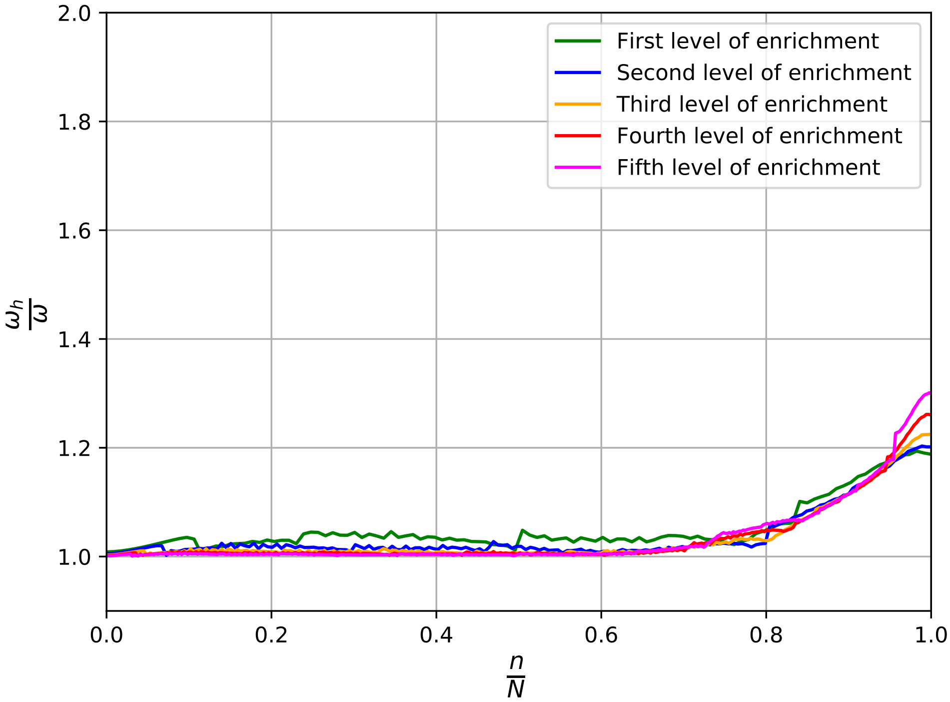

Figure 4. Enrichment Arndt [15] for beams

For a better observation, a zoom at the end of the spectrum is presented in Fig. 5.

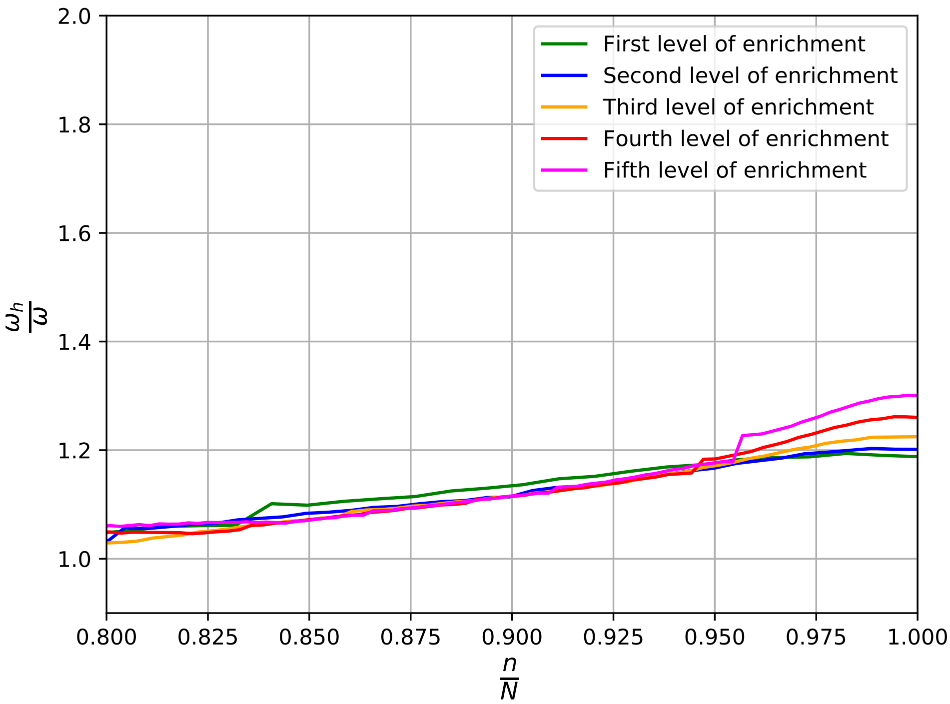

Figure 5. Zoom of enrichment Arndt [15] for beams

For this enrichment the increase in the level of enrichment is not so beneficial to the model of

Timoshenko. In the Fig. 5, it can be seen that the fifth level of enrichment has the best responses to close to 83% up to 95% of the frequencies, while for the other frequencies presented in this same Fig. the fifth level of enrichment presents the results farthest from the reference solution.

The spectrum, shown in Fig. 6, is for the set of enrichment functions presented by Hsu [22] for beams.

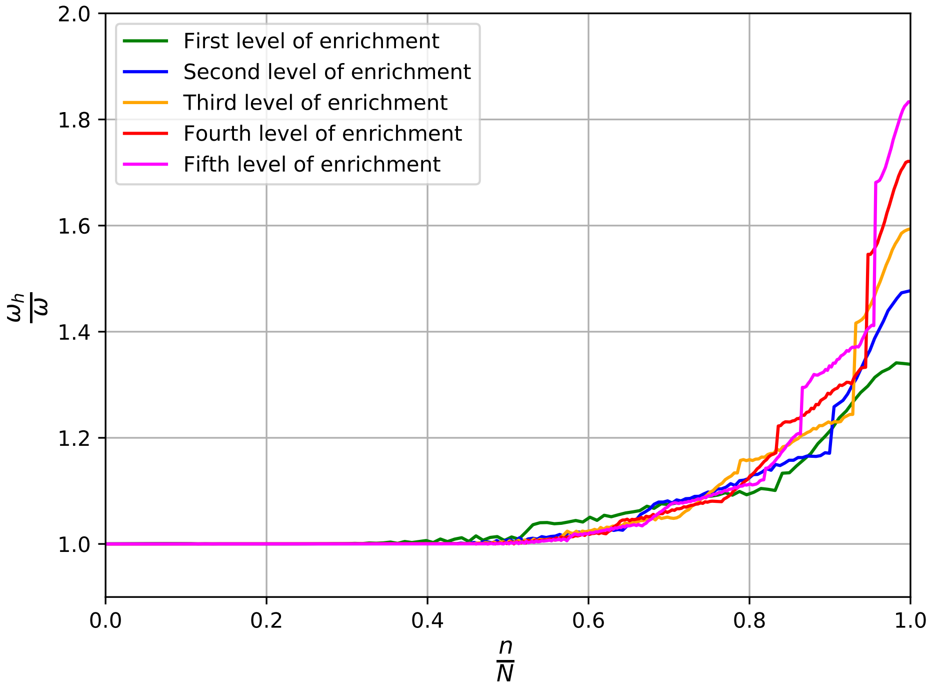

Figure 6. Enrichment Hsu [22] for beams

For a better observation, a zoom at the end of the spectrum is presented in Fig. 7.

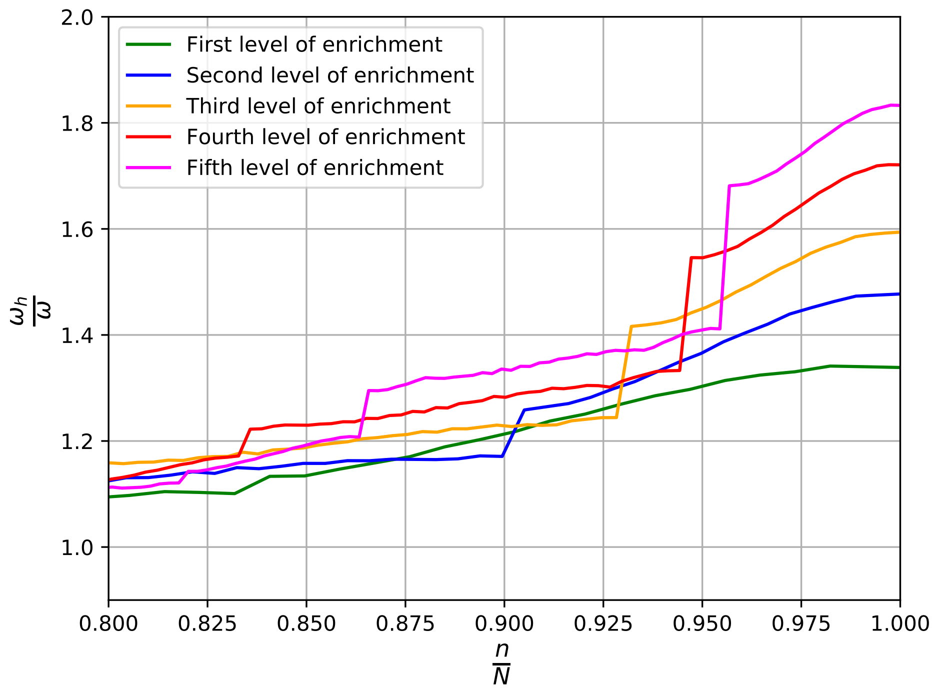

Figure 7. Zoom of enrichment Hsu [22] for beams

The frequencies found with the first level of enrichment obtained the best responses than to the fifth level of enrichment, as can be seen in the Fig. 7.

In order to compare the three enrichments, a frequency spectrum graph with the FEM response and the fifth level of enrichment for the three GFEM enrichment function sets is presented in the Fig. 8.

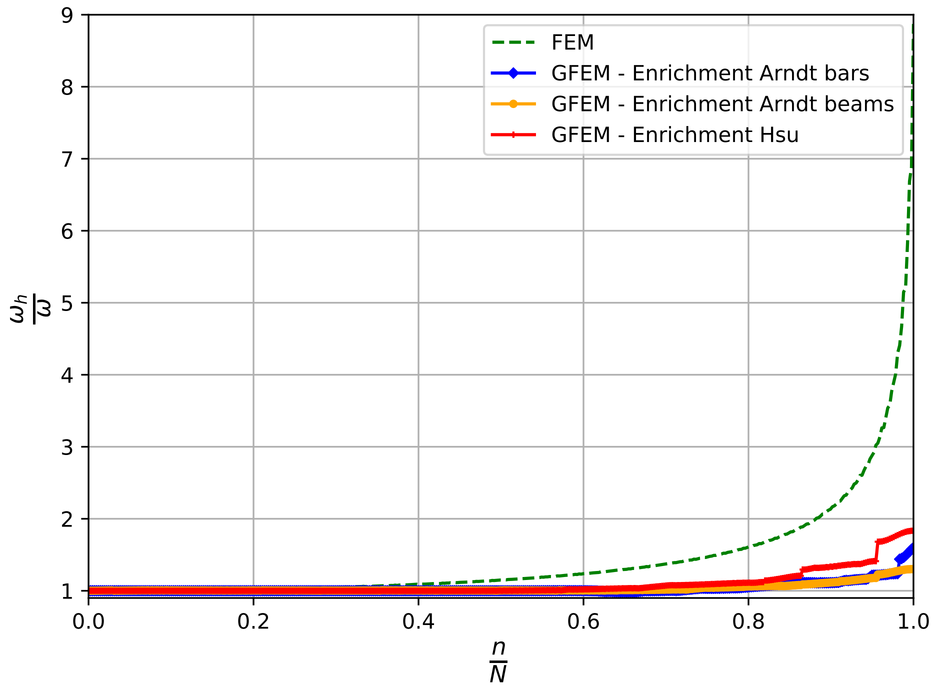

Figure 8. Fifth level of enrichment

For a better observation, a zoom at the end of the spectrum is presented in Fig. 9.

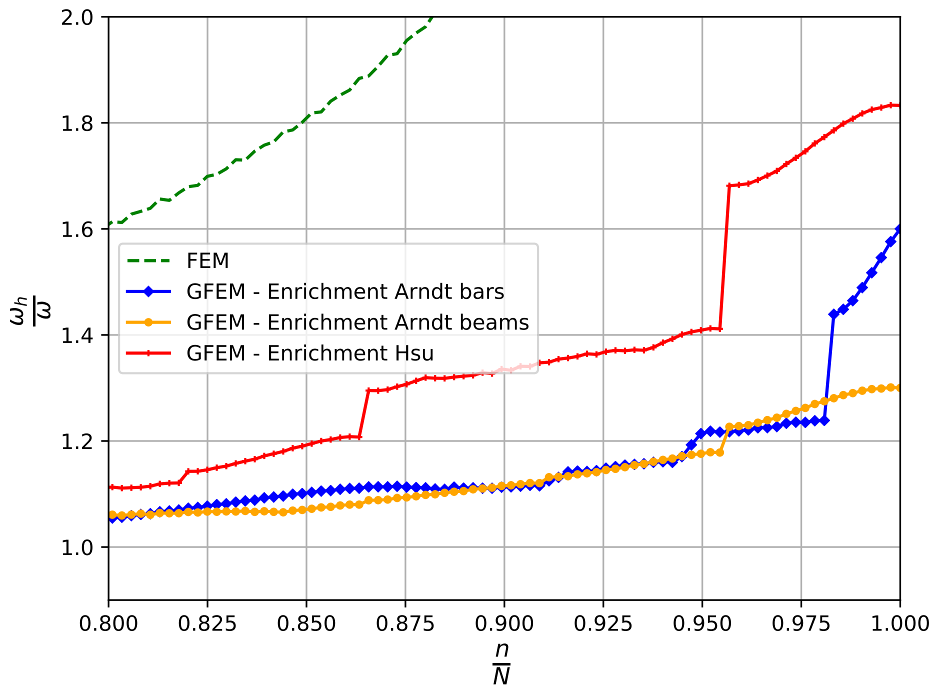

Figure 9. Zoom of fifth level of enrichment

The responses presented by the three GFEM enrichments are better than the FEM response. The frequencies of FEM begin to distance themselves from the reference response from 40% of the frequencies, whereas for the three enrichments it occurs only from 80%. Comparing the three different enrichments of GFEM in Fig. 9, one can conclude that the Arndt [15] enrichments for bars and beams have the best answers for this example.

Table 1 shows the first 15 dimensionless eigencalues β_n, so that it is possible to compare the results obtained by GFEM enrichments with the results of different authors and methods. GFEM results were obtained using three enrichment levels, the FEM results are from the reference solution and from HFEM are taken from the (Hsu2016) with the employment of 6 enriching functions and 10 elements.

In Table 1 one can see that the results obtained with the three enrichments are close to the results obtained by other authors. The enrichment of Arndt [15] for bars presents results lower than those obtained by FEM, results that are the same as those obtained by HFEM, so they are presumably more accurate. Thus, analyzing only the table for the first 15 eigenvalues the enrichment of Arndt [15] for bars is the best among the three enrichments.

In order to be able to evaluate the convergence of the different enrichments used, in order to compare the performance and the convergence rate of the set of enriching functions, the graphs on Fig. 10 and Fig. 11 are presented with the evolution of the relative errors of some frequencies. The value of the error is obtained by Arndt [15]:

$$error = 100\frac{\mid \omega_n - \omega \mid}{\omega}(\%). \tag{34}$$

The graphs obtained with the relative error are shown in the Fig. 10 and Fig. 11. The first shows the relative errors for the first frequency and the second presents the relative errors for the second frequency.

The relative error presented for the first two frequencies, considering the enrichment of Arndt [15] for bars and Hsu [22] are similar. The enrichment of Hsu [22] shows a higher convergence rate for the first frequency. The enrichment of Arndt [15] for beams seems to presents higher error values, and also a low convergence rate, but to be a monotonic convergence.

Table 1. Dimensionless eigenvalues β_n

Modes	FEM	HFEM [22]	Isog. Analysis [26]	GFEM - [15] for bars	GFEM - [15] for beams	GFEM - [22]
1	1,867714	1,867714	1,8677	1,867715	1,872548	1,867715
2	4,572409	4,572408	4,5724	4,572410	4,585042	4,572411
3	7,415417	7,415415	7,4154	7,415419	7,438700	7,415419
4	9,987355	9,987350	9,9874	9,987355	10,024300	9,987357
5	12,322442	12,322432	12,3224	12,322439	12,376532	12,322442
6	14,445910	14,445893	14,4459	14,445900	14,520763	14,445906
7	16,388350	16,388325	16,3883	16,388332	16,487471	16,388340
8	18,176654	18,176619	18,1767	18,176626	18,303226	18,176637
9	19,832883	19,832836	19,8330	19,832841	19,989543	19,832855
10	21,374112	21,374051	21,3743	21,374054	21,562664	21,374072
11	22,812558	22,812481	22,8130	22,812485	23,033447	22,812502
12	24,153727	24,153634	24,1546	24,153635	24,404440	24,153654
13	25,387630	25,387523	25,3892	25,387523	25,654369	25,387541
14	26,218679	26,218657	26,2191	26,218657	26,255349	26,218660
15	26,555938	26,555856	26,5577	26,555856	26,738758	26,555866

The condition numbers of the matrices for each example will also be evaluated. The condition number of a matrix A, denoted as $C(A)$, provides an estimate of the number of precision digits required in solving equations such as Eq. (15). The condition number is the ratio of the largest to the smallest eigenvalue of the matrices. The closer to the unit the greater the stability of the method [28]. The condition number according to Bazan [29] is given by:

$$C(A) = \| A \| \| A^{-1} \|, \tag{35}$$

where the norm used in this work is the Euclidian.

The Fig. 12 and Fig. 13 show the condition number plots of the stiffness and mass matrices, respectively.

In the graphs, the FEM matrices have better condition numbers for the first 10 levels of enrichment. The Arndt [15] enrichment condition numbers for bars vary greatly from the highest to the lowest. Among the other two enrichments, the Hsu [22] has the most well-conditioned matrices.

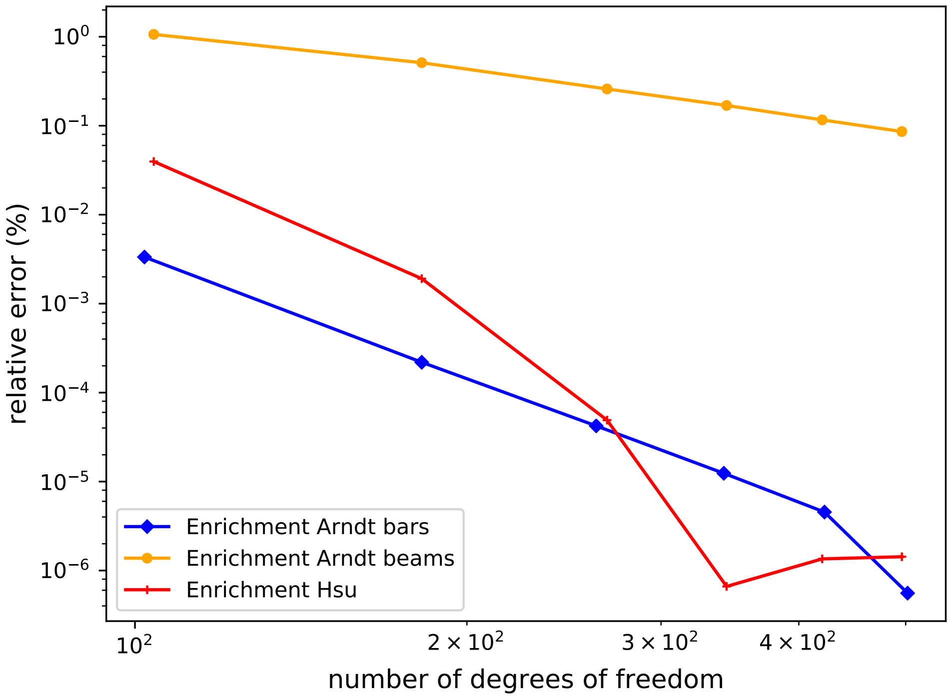

Figure 10. Graphics of convergence for the first frequency

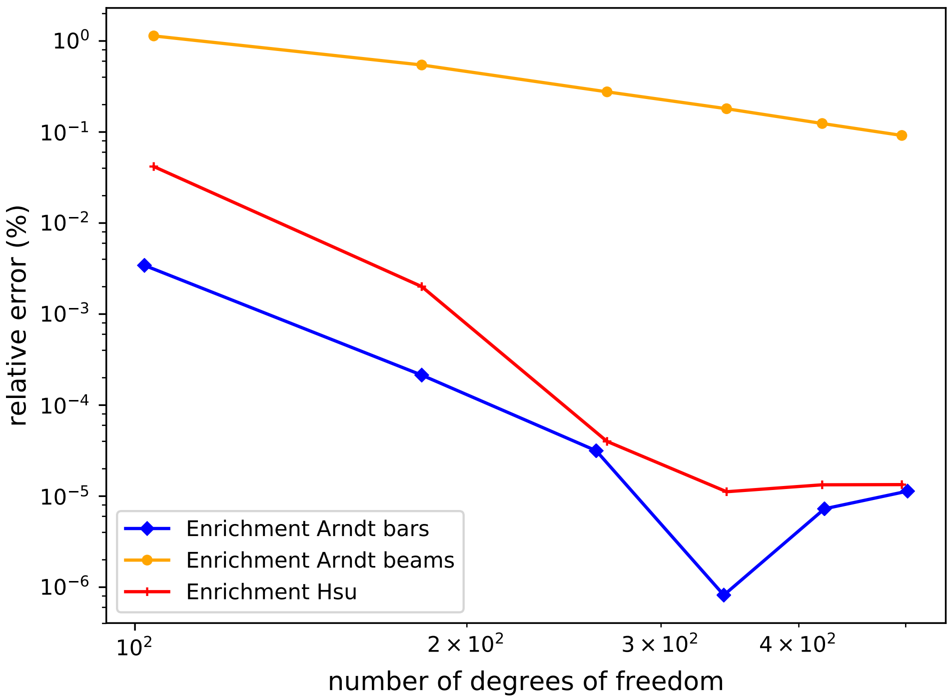

Figure 11. Graphics of convergence for the second frequency

4.2 Transient analysis

For the transient analysis it was chosen a beam with a relationship between the cross-sectional height and the beam length of 0.2.

For time discretization, the study time interval is 200 seconds, which was analyzed in steps of 10^{-2}

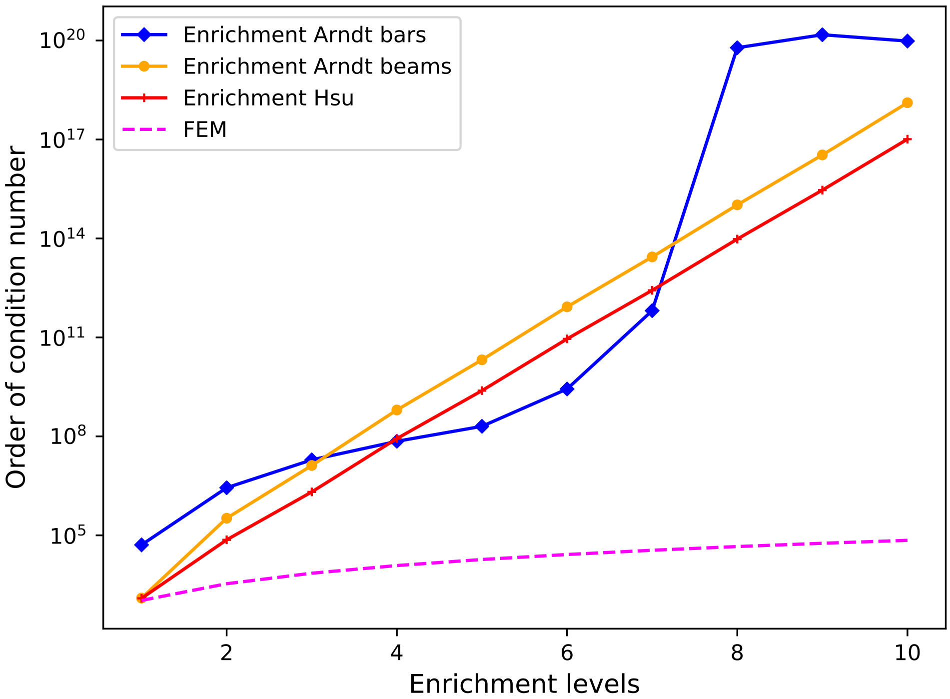

Figure 12. Graphics of the condition number of the stiffness matrices

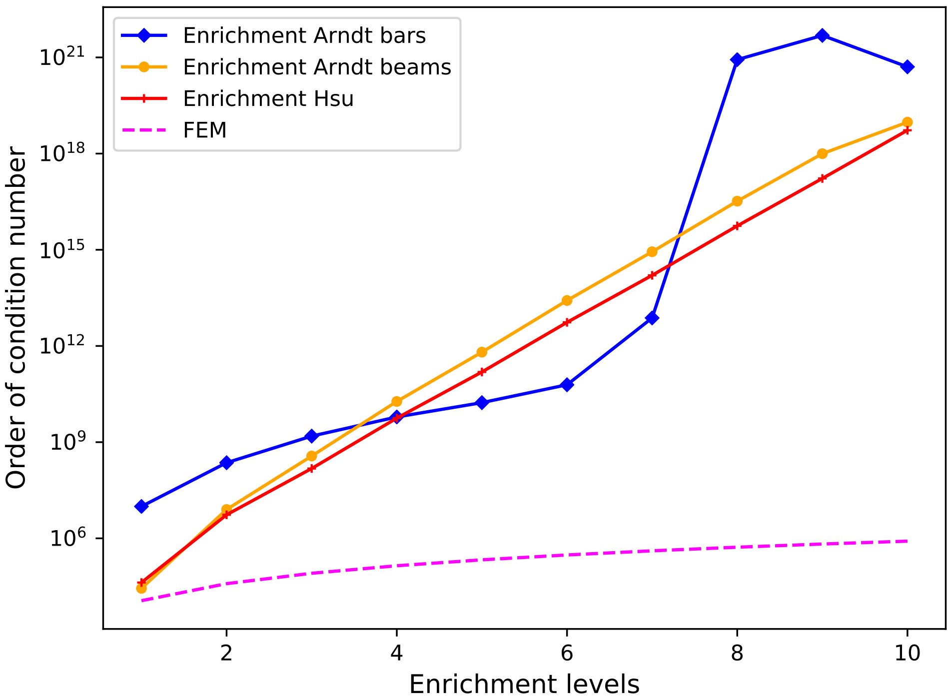

Figure 13. Graphics of the condition number of the mass matrices

seconds. To provide better visibility of responses, the time interval shown in some figures is smaller. For the integration in time was used the method of Newmark. The graphs are relative to the free end node. An external step-type excitation of $1\ N$ is applied at the free end of the beam. A model with 8000 degrees of freedom was adopted as reference solution validating a sufficiente reliabe reference.

The Fig. 14 and Fig. 15 show the displacement responses with one and five enrichment levels, respectively, they also show a zoom so that the behavior of the enrichments can be observed in more detail.

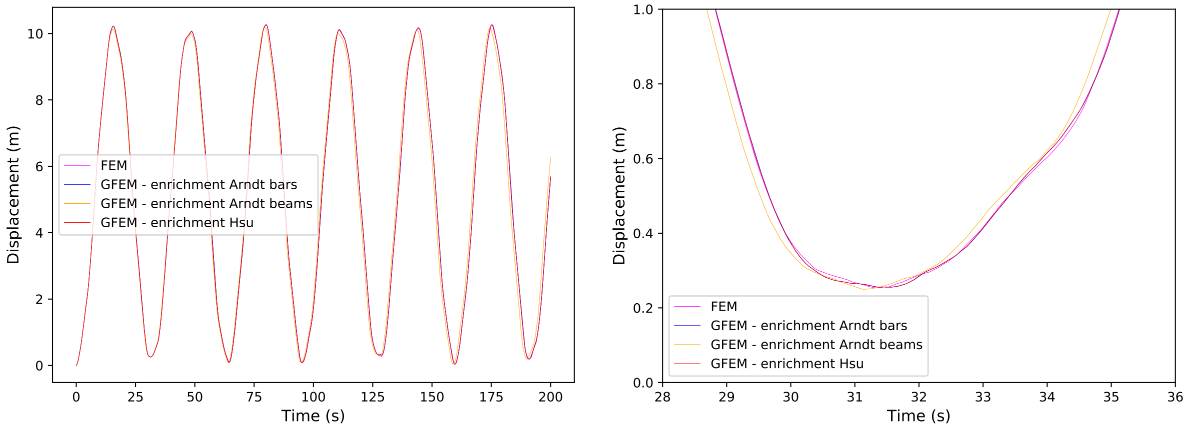

Figure 14. Transient response in displacement terms with one level of enrichment.

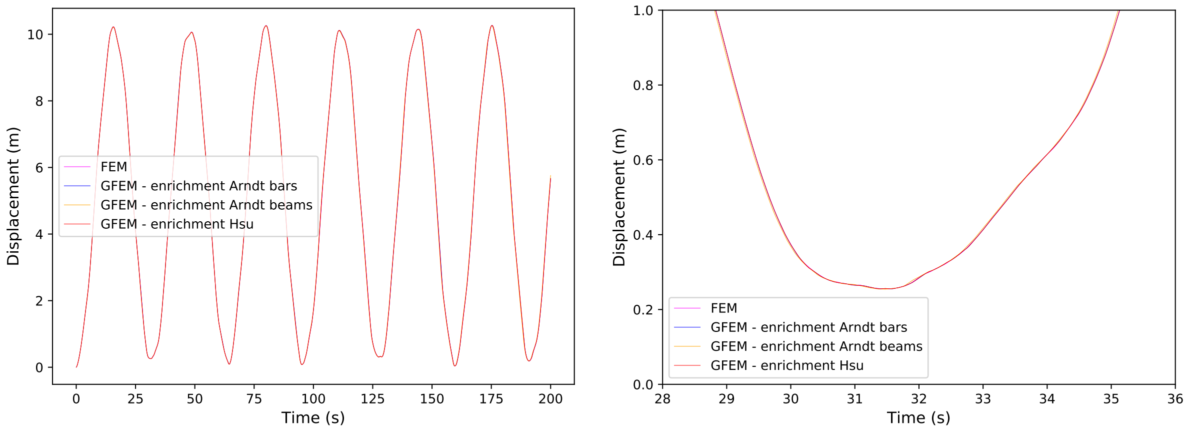

Figure 15. Transient response in displacement terms with five levels of enrichment.

In the Fig. 14 it can be seen that Arndt [15] enrichment for beams is not the most accurate. However, by increasing the level of enrichment the curves are very similar. The other enrichments present results almost equal to those of FEM, being difficult to perceive the difference between them.

Figure 16 and Fig. 17 show the velocity responses with one and five enrichment levels, respectively.

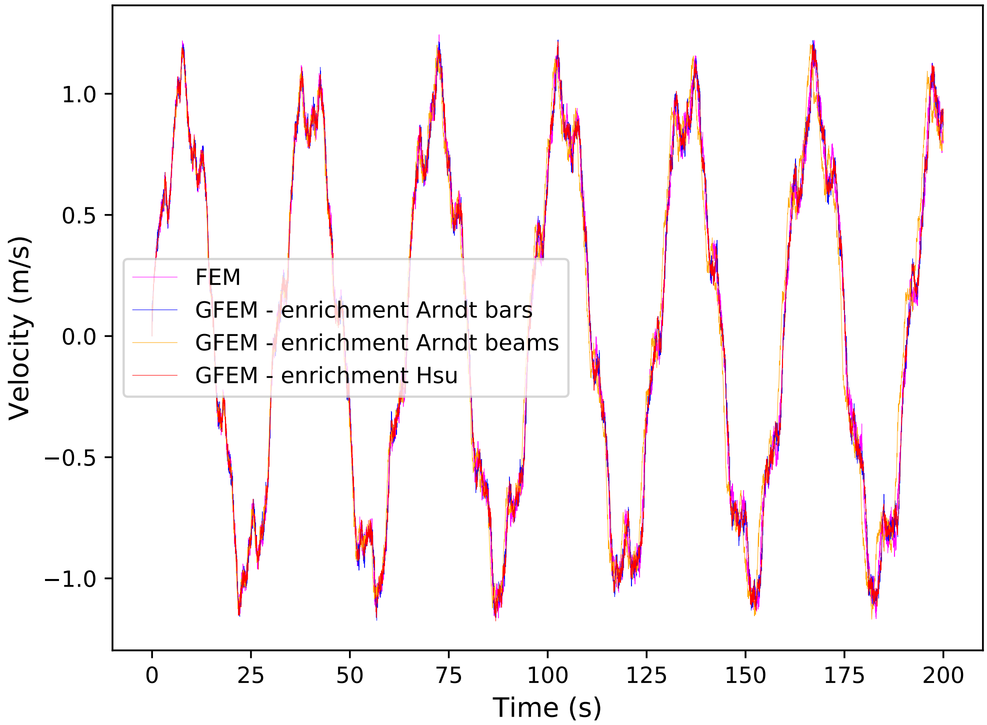

Figure 16. Transient response in velocity terms with one level of enrichment.

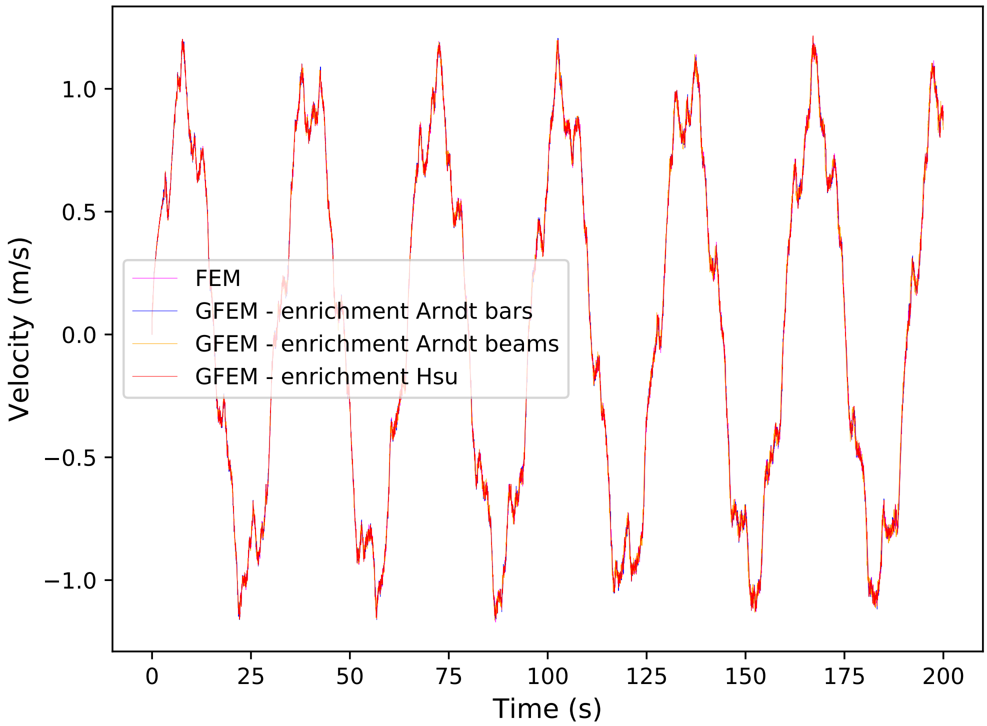

Figure 17. Transient response in velocity terms with five levels of enrichment.

The behavior of the four velocity curves is similar. Even if they do not show the same results it is difficult to distinguish which enrichment behaved more efficiently.

Figure 18 and Fig. 19 show the acceleration responses with one and five enrichment levels, respectively.

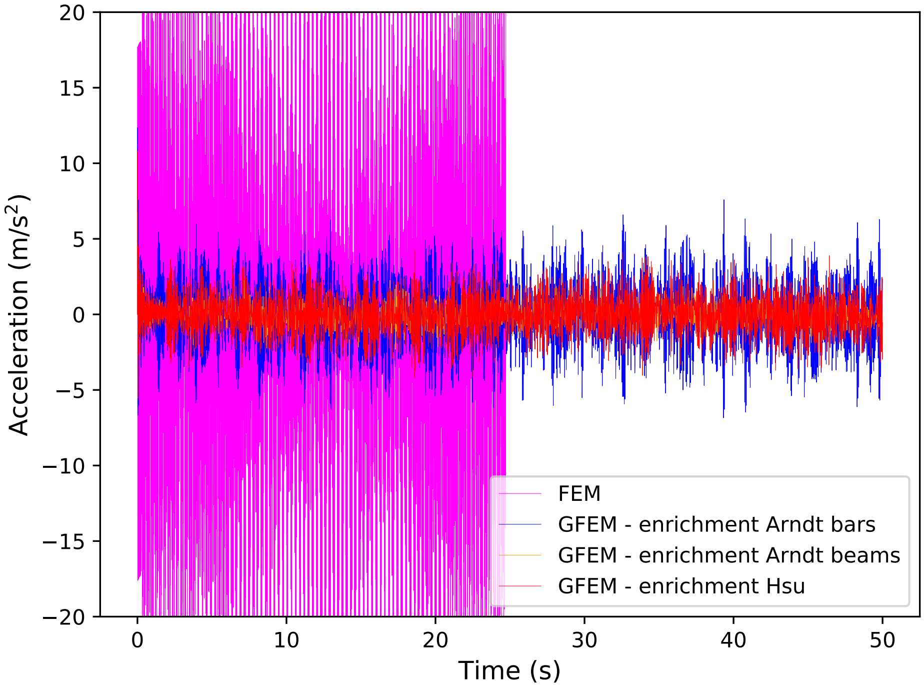

Figure 18. Transient response in acceleration terms with one level of enrichment.

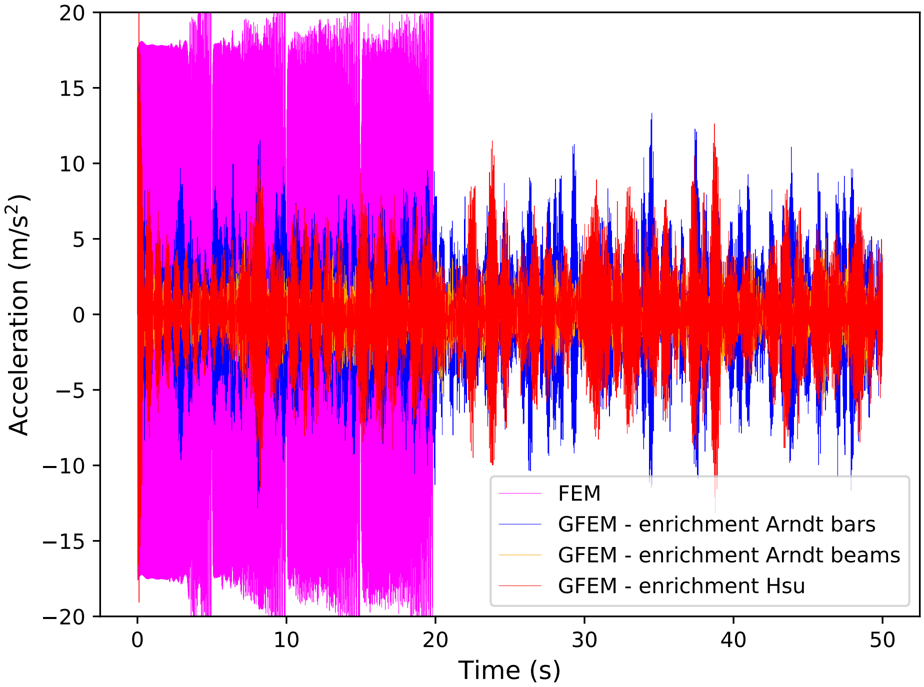

Figure 19. Transient response in acceleration terms with five levels of enrichment.

The acceleration results of FEM have higher peaks than GFEM, but the values of these peaks decrease with increasing degrees of freedom. However, for the GFEM results the opposite is the result, as there is an increase in the number of degrees of freedom there is an increase in the peak values of the acceleration responses.

5 Concluding remarks

This work aimed to apply the GFEM to dynamic analysis of Timoshenko beams and to analyze the behavior of different sets of trigonometric enrichment functions. The enrichments were presented in the following order, the first enrichment presented was that shown in Arndt [15] for bars, with modifications proposed by Torii [2] and Weinhardt [17]. The second enrichment was also presented in the work of Arndt [15] for Euler-Bernoulli beams. The last enrichment used was presented in the work of Hsu [22], already employed in Timoshenko beams. This work compiled all these strategies and presented insightfull discussion that may guide further researches.

In order to perform the modal analysis and to compare the three different enrichments, applied with the GFEM, with FEM, a clamped-free beam with a ratio between the cross-sectional height and the beam length of 0.1 was chosen. Frequency spectrum were obtained, comparing the enrichment functions with FEM. The spectra results indicated that the enrichment of Arndt [15] for beams obtains better results than the others, thus following the enrichment of Arndt [15] for bars. This result brings new perpectives to the subject, thus contributing to the field.

A table was then presented in which the GFEM results with three enchment levels were compared with the results obtained by other authors and FEM. It was concluded that the results obtained with the three trigonometric enrichments were similar to those obtained by other authors. The results that presented a greater precision were obtained with the enrichment of Arndt [15] for bars, followed by the enrichment of Hsu [22]. A question left over in this aspect consists in studying numerical stability issues, following research trends in the application o GFEM to Dynamics.

The convergence plots showed that the enrichment of Arndt [15] for beams has a high relative error for this example and a low convergence rate for the first two frequencies, which is not possible to observe in the frequency spectra. The other two enrichments presented, at the highest enrichment level, very close error values. The rate of convergence of the enrichment of Hsu [22] was higher but the enrichment of Arndt [15] for bars although with lower convergence rate was more accurate, suggesting that new enrichment strategies may be proposed aiming an optimized procedure.

A preliminary numerical statility analysis of the matrices was presented using the condition number as a representative measure. The condition number of mass and stiffness matrices were presented showing that the matrices related to Hsu [22] enrichment are more stable. This result incorporates a contribution to the discussion and aims to foment new discussion branches featuring numerical stability.

For the transient analysis, a clamped-free beam was chosen as main example. Three different enrichments and their results were compared to those obtained with FEM analysis. The transient analysis responses were presented in terms of displacement, velocity and acceleration. FEM already has very accurate results for displacements and the enrichment does not improve approximation greatly. Another aspect worth highlighting is the fact that the three enrichments present similar results, always very similar to the FEM solution. Thus, for the transient analysis it is not possible to highlight or discard any of the enrichments, it was only possible to observe that they have good application for the transient analysis of Timoshenko beams as well.

As a main observation, it's interesting to sumarize that two enrichments presented good results for the example. The enrichment of Arndt [15] for bars obtained a better overall frequency spectrum, while the convergence plots pointed to a higher convergence rate for Hsu [22] enrichment. Enrichment of Hsu [22] also presents condition number lower than the enrichment of Arndt [15] for bars, for the higher levels. Finally, the discussion is open and further investigations may follow threads presented in this paper.

References

[1] Rao, S. S., 2011. *Mechanical Vibrations*. Pearson, 5th edition.

[2] Torii, A. J., 2012. *Análise dinâmica de estruturas com o Método dos Elementos Finitos Generalizado*. PhD thesis, Universidade Federal do Paraná, Curitiba.

[3] Chopra, A. K., 2011. *Dynamics of Structures*. Pearson, fourth edition.

[4] Becker, E. B., Carey, G. F., & Oden, J. T., 1981. *Finite Elements: An Introduction*, volume I. Prentice Hall.

[5] Bathe, K., 1982. *Finite Element Procedures in Engineering Analysis*. Prentice Hall.

[6] Hughes, T. J. R., 1987. *The Finite Element Method: Linear Static and Dynamic Finite Element Analysis*. Prentice Hall.

[7] Bellman, R. & Casti, J., 1971. Differential quadrature and long-term integration. *Journal of Mathematical Analysis and Applications*, vol. 34, pp. 235–238.

[8] Jang, S. K., Bert, C. W., & Striz, A. G., 1989. Application of differential quadrature to static analysis of structural components. *International Journal of Numerical Methods in Engineering*, vol. 28, pp. 561–577.

[9] Hughes, T. J. R., Cottrell, J. A., & Bazilevs, Y., 2005. Isogeometric analysis: Cad, finite elements, nurbs, exact geometry and mesh refinement. *Computer Methods in Applied Mechanics and Engineering*, vol. 194, pp. 4135–4195.

[10] Palazzolo, A., 2016. *Vibration Theory and Applications with Finite Elements and Active Vibration Control*. Wiley, Texas.

[11] Bhavikatti, S. S., 2005. *Finite element analysis*. New Age International (P) Limited.

[12] Melenk, J. M., 1995. *On generalized finite element methods*. PhD thesis, Faculty of the Graduate School of The University of Maryland, Maryland.

[13] Melenk, J. M., 1992. Finite element methods with harmonics shape functions for solving laplace's equation. Master's thesis, Faculty of the Graduate School of the University of Maryland, Maryland.

[14] Strouboulis, T., Babuška, I., & Copps, K., 2000. The design and analysis of the generalized finite element method. *Computer Methods in Applied Mechanics and Engineering*, vol. 181, pp. 43–69.

[15] Arndt, M., 2009. *O Método dos Elementos FInitos Generalizados aplicado à Análise de vibrações livres de estruturas reticuladas*. PhD thesis, Universidade Federal do Paraná, Curitiba.

[16] Shang, H. Y., 2014. *Análise dinâmica elastoplástica de problemas da mecânica de sólidos via métodos enriquecidos de elementos finitos*. PhD thesis, Pontifícia Universidade Católica do Paraná, Curitiba.

[17] Weinhardt, P. d. O., 2016. Estudo da estabilidade do método dos elementos finitos generalizados aplicado à análise dinâmica. Master's thesis, Universidade Federal do Paraná, Curitiba.

[18] Petroli, T., 2016. Condicionamento do problema de autovalores obtido do método de elementos finitos generalizados na dinâmica de estruturas. Master's thesis, Universidade Federal do Paraná, Curitiba.

[19] Debella, L. B. C., 2018. Análise dinâmica transiente pelo método dos elementos finitos generalizados. Master's thesis, Universidade Federal do Paraná, Curitiba.

[20] Malacarne, M. F., 2018. O indicador de erro de friberg empregado no método dos elementos finitos generalizados aplicado à análise dinâmica de estruturaas. Master's thesis, Universidade Federal do Paraná, Curitiba.

[21] Corrêa, R. M., 2019. Análise dinâmica de arcos usando o método dos elementos finitos generalizados. Master's thesis, Universidade Federal do Paraná, Curitiba.

[22] Hsu, Y. S., 2016. Enriched finite element methods for timoshenko beam free vibration analysis. *Applied Mathematical Modelling*, vol. 40, pp. 7012–7033.

[23] Freisleben, P. L. M., Arndt, M., de Oliveira Weinhardt, P., & Machado, R. D., 2017. Dynamic analysis of timoshenko beams using the generalized finite element method. In Faria, P., Lopez, R., Miguel, L., Gomes, W., & Noronha, M., eds, *XXXVIII Iberian Latin-American Congress on Computational Methods in Engineering*, Florianópolis, SC. ABMEC.

[24] Freisleben, P. L. M., 2019. Análise dinâmica de vigas de timoshenko utilizando o método dos elementos finitos generalizados. Master's thesis, Universidade Federal do Paraná, Curitiba.

[25] Timoshenko, S. P., 1921. Lxvi. on the correction for shear of the differential equation for transverse vibrations of prismatic bars. *The London, Edinburgh, and Dublin Philosophical Magazine and Journal of Science*, vol. 41, n. 245, pp. 744–746.

[26] Lee, S. J. & Park, K. S., 2013. Vibrations of timoshenko beams with isogeometric approach. *Applied Mathematical Modelling*, vol. 37, n. 22, pp. 9174–9190.

[27] Arndt, M., Torii, A. J., Machado, R. D., & Scremin, A., 2014. Generalized finite element method for vibration alalysis of bars. In *10th World Congress on Computational Mechanics*, volume 1, São Paulo. Blucher Mechanical Engineering Proceedings.

[28] Cook, R. D., Malkus, D. S., Plesha, M. E., & Witt, R. J., 2001. *Concepts and Applications of Finite Element Analysis*. John Wiley & Sons, Inc., 4th edition.

[29] Bazan, F. S. V., 2003. Autovalores de polinômios matriciais: Sensibilidade, computação e aplicações.